European Journal of Radiology Open 8 (2021) 100367

Contents lists available at ScienceDirect

European Journal of Radiology Open

journal homepage: www.elsevier.com/locate/ejro

Assessing the value of volume navigation during ultrasound-guided radiofrequency- and microwave-ablations of liver lesions

Philippa Meershoek [a,b], Nynke S. van den Berg [b], Jacob Lutjeboer [a], Mark C. Burgmans [a], Rutger W. van der Meer [a], Catharina S.P. van Rijswijk [a], Matthias N. van Oosterom [b], Arian R. van Erkel [a], Fijs W.B. van Leeuwen [b,*]

[a] Interventional Radiology Section, Department of Radiology, Leiden University Medical Center, Albinusdreef 2, 2300 RC, Leiden, the Netherlands
[b] Interventional Molecular Imaging Laboratory, Department of Radiology, Leiden University Medical Center, Albinusdreef 2, 2300 RC, Leiden, the Netherlands

ARTICLE INFO

Keywords:
Radiofrequency ablation
Microwave ablation
Image guided interventions
Interventional radiology
Navigation
Ultrasound

ABSTRACT

Purpose: The goal of our study was to determine the influence of ultrasound (US)-coupled volume navigation on the use of computed tomography (CT) during minimally-invasive radiofrequency and microwave ablation procedures of liver lesions.

Method: Twenty-five patients with 40 liver lesions of different histological origin were retrospectively analysed. Lesions were ablated following standard protocol, using 1) conventional US-guidance, 2) manual registered volume navigation (*m*VNav), 3) automatic registered (*a*VNav) or 4) CT-guidance. In case of ultrasonographically inconspicuous lesions, conventional US-guidance was abandoned and *m*VNav was used. If *m*VNav was also unsuccessful, the procedure was either continued with *a*VNav or CT-guidance. The number, size and location of the lesions targeted using the different approaches were documented.

Results: Of the 40 lesions, sixteen (40.0 %) could be targeted with conventional US-guidance only, sixteen (40.0 %) with *m*VNav, three (7.5 %) with *a*VNav and five (12.5 %) only through the use of CT-guidance. Of the three alternatives (*m*VNav, *a*VNav and CT only) the mean size of the lesions targeted using *m*VNav (9.1 ± 4.6 mm) was significantly smaller from those targeted using US-guidance only (20.4 ± 9.4 mm; $p < 0.001$). The location of the lesions did not influence the selection of the modality used to guide the ablation.

Conclusions: In our cohort, *m*VNav allowed the ablation procedure to become less dependent on the use of CT. *m*VNav supported the ablation of lesions smaller than those that could be ablated with US only and doubled the application of minimally-invasive US-guided ablations.

1. Introduction

The success of radiofrequency (RFA) and microwave ablation (MWA) procedures is directly dependent on accurate lesion localization and applicator placement. To guide applicator placement, RFA and MWA procedures are generally performed under image guidance of ultrasound (US), computed tomography (CT) or magnetic resonance (MR) imaging [1,2]. Of the three technologies US-guidance is most practical; The real-time image guidance provided by US enables beginning to end monitoring of the procedure and when required allows for adaptation of the electrode insertion path at lower costs compared to the other imaging modalities [3,2,4–8]. However, lesions can be inconspicuous on US as a consequence of e.g. isoechogenicity, small size, subphrenic localization, (macronodular) cirrhosis, or patient habitus [2,3,9–11]. In fact, Rhim et al. [12] reported that the inability to visualize lesions on US accounted for 55.8 % of the lesions that could not be ablated using conventional US-guidance.

A possibility to overcome this shortcoming is the use of navigation in three-dimensional (3D) pre-interventional imaging data sets. Navigation approaches help overcome all kinds of shortcomings of interventional imaging modalities such as fluorescence imaging, gamma-ray guidance, and US [13–18]. For the latter, volume based navigation (VNav) can be realized by manual and/or automatic co-registration of US-images with (pre-)interventional acquired CT- or MR-imaging data sets [19–22].

* Corresponding author at: Interventional Molecular Imaging Laboratory Department of Radiology Leiden University Medical Center (LUMC) Albinusdreef 2, PO Box 9600, postal zone C2-S, 2300 RC, Leiden, the Netherlands.
E-mail address: F.W.B.van_Leeuwen@lumc.nl (F.W.B. van Leeuwen).

https://doi.org/10.1016/j.ejro.2021.100367
Received 28 April 2021; Received in revised form 25 June 2021; Accepted 30 June 2021

Although the technology is being implemented, few studies have reported on the technical feasibility of this approach [8,15,23]. This particular study focused on establishing how manual registered volume navigation (*m*VNav) could help reduce the usage of interventional CT during US-guided ablations of liver lesions.

2. Material and methods

2.1. Patients

All patients scheduled for an ablation procedure of liver lesions between August 2015 and February 2016 were retrospectively included in the study after obtaining written informed consent. This study was conducted in accordance to the 1964 Helsinki Declaration and its later amendments, and received a certificate of no objection by the Medical Ethical Committee of our institute.

25 patients with, in total, 40 lesions were included: 23 hepatocellular carcinomas (HCC), 11 colorectal metastases, four bronchocarcinoid metastases and two (choroideal) melanoma metastases. Demographic, liver and lesion specific information is presented in Table 1. Liver cirrhosis and the aetiology of the cirrhosis were evaluated next to the type, size (largest diameter measured on the most recent CT- or MR-imaging) and location of the lesion.

2.2. Pre- and post-interventional imaging

Diagnosis of the lesion type was based on imaging (n = 22 patients) or biopsy histology (n = 3 patients). The CT- and MR-images that provided the basis for navigation were derived from diagnostic multiphase contrast-enhanced CT (CE-CT) or dynamic gadolinium-enhanced MRI scans [24].

A contrast-enhanced CT-scan (CE-CT) was performed on an Aquilion 16 (Toshiba Medical Systems, Otawara, Japan) after the ablation procedure (in the same session; Fig. 1). Technical success was defined as described by Ahmed et al. [25].

2.3. Navigation hardware

The Logiq E9 with XDclear (General Electric (GE) Healthcare, Little Chalfont, Buckinghamshire, United Kingdom) US system was used and combined with a driveBAY™ (Ascension Technology Corp. an NDI company, Shelburne, Vermont, USA). This system was equipped with a mid-range electromagnetic transmitter (Ascension Technology Corp.; Fig. 1). On the C1−6-D transducer (GE Healthcare) a VNav tracking bracket (Civco Medical Solutions, Coralville, Iowa, USA) was placed, to which general-purpose electromagnetic sensors (Civco Medical Solutions) were coupled. These sensors were then connected to the driveBAY™, allowing the 3D spatial registration of the location of the transducer within the magnetic field.

To steer the applicator or support needle towards the region of interest on the ultrasound transducer an In-Plane Ultrasound Needle Guide – Ultra-Pro™ (Civco Medical Solutions) was attached and combined with the Ultra-Pro II™ needle guidance system (Civco Medical Solutions).

For manual registered volume navigation (*m*VNav) the 3D pre-interventional images were manually co-registered to the real-time US by establishing a lock on an anatomical plane based on landmarks (hereafter referred to as plane-lock), visible on both the US and the pre-interventional images, as described in Burgmans et al. [23]. After the plane-lock was set, further manual refinement of the co-registration was performed by selecting specific landmarks visible on US as well as on the CT or MR-images.

For automatic registered volume navigation (*a*VNav) an omniTRAX™ active patient tracker (Civco Medical Solutions) (Fig. 1, white arrow) was placed on a solid part of the body of the patient (e.g. sternum) after which a CE-CT scan was made during the intervention. These CE-CT-images were downloaded into the US system. A general purpose electromagnetic sensor was connected to the active patient tracker and the driveBAY™. Via the auto-registration software option, which recognises the orientation of the active tracker in both the acquired CE-CT-scan and on the patient, the acquired CE-CT-images were coupled to the US-images.

2.4. Ablation hardware

The Cool-tip™ RF ablation system E Series and corresponding three or four cm exposure electrodes (Covidien, Medtronic, Minneapolis, Minnesota, USA) and the HS Amica™ with corresponding antennas (HealthTronics, Austin, TX, USA) were used for RFA and MWA procedures, respectively. The ablation system used depended on the operator's preference and e.g. nearby located structures that could induce the heat sink effect.

2.5. Ablation procedure

All interventions were performed in the CT intervention suite under general anaesthesia (Fig. 1) by four experienced interventionalists. A schematic overview of the navigated RFA/MWA procedure is given in Fig. S1. For the analysis a scoring system of two points was used to classify the certainty of the localization of each separate lesion: "visible and/or certain enough to place the electrode" (1) and "not visible" or "not certain of the localization" (2).

If the lesion was visible with conventional US (score 1), the RFA or MWA applicator was placed under US-guidance followed by ablation. If the lesion was not visible on conventional US or the lesion localization was uncertain (score 2), the navigation function of the US system was turned on and the procedure was continued using *m*VNav. Again the visibility and certainty of lesion localization were determined using the above-mentioned two-point scoring system. If score 1, the electrode was placed in the lesion and the ablation was performed. If score 2, the interventionalist could continue with either 1) *a*VNav, or 2) abandon the navigation approach and use CT-guidance for applicator placement. When *a*VNav was used and the lesion was still not visible, or when the interventionalist was still uncertain (score 2), the ablation procedure was performed using CT-guidance.

The following data were collected for each lesion: the visibility of the lesion, certainty of having localized the lesion, position of the patient, images for navigation (modality, phase, thickness and date), number of used landmarks and their location, and number of ablation electrodes (depending on the estimated ablation zone given by the guideline of the ablation equipment and the size and location of the lesion).

Table 1
Patient and lesion characteristics.

Characteristics	
Patients (n = 25 (100 %))	
- Mean age ± SD (range)	- 65 ± 10.9 (43–81)
- Male	- 17 (68.0 %)
- Female	- 8 (32.0 %)
Patients with liver cirrhosis (n = 13 (52.0 %))	
- Cryptogenic	- 2 (8.0 %)
- Hepatitis B	- 1 (4.0 %)
- Hepatitis C	- 5 (20.0 %)
- Alcoholic	- 5 (20.0 %)
Lesions (n = 40 (100 %))	
- Median of lesions per patient (range)	- 1 (1–4)
- HCC	- 23 (57.5 %)
o Mean size ± SD (mm)	o *16.8 ± 7.9*
- Metastases	o 17 (42.5 %)
o Mean size ± SD (mm)	- *13.7 ± 9.6*

n = amount; SD = standard deviation; HCC = hepatocellular carcinoma; mm = millimeter.

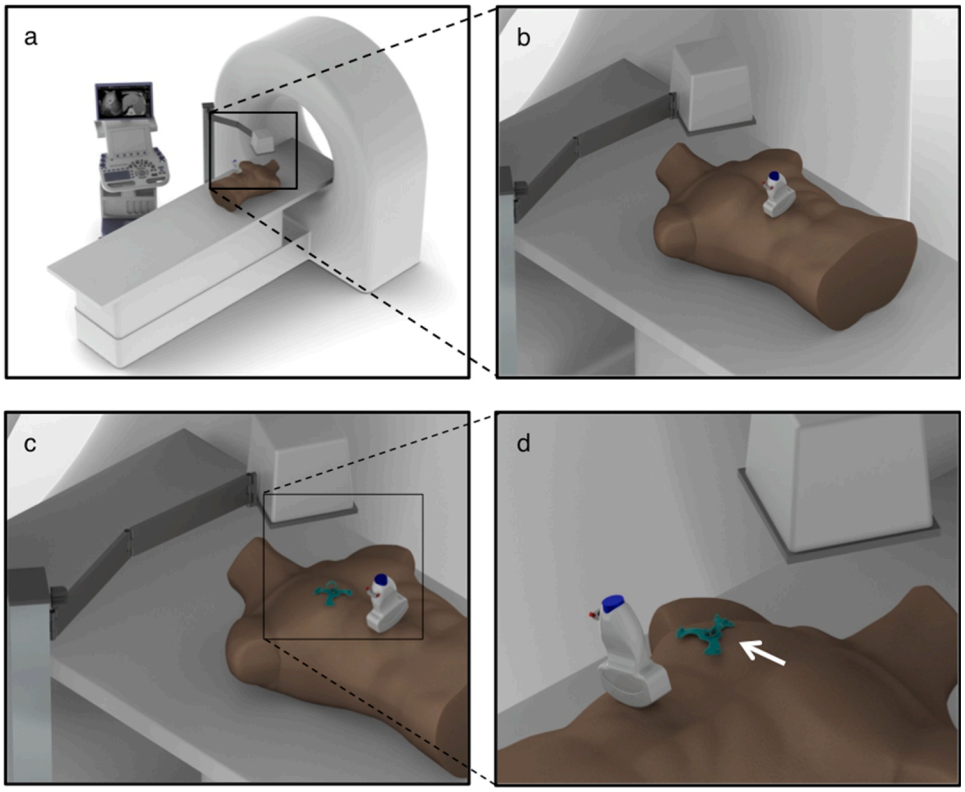

Fig. 1. US-based navigation setup. (a) The setup of the CT intervention suite with US system and electro magnet. The setup for manual registered VNav is shown in (b) and automatic registered VNav in (c) with the active tracker placed on the patient. The magnet has to be placed near the workfield to track the sensors attached to the transducer and active tracker (arrow)(d).

2.6. VNav error measurements

During navigation a lesion could become visible on US to the interventionalist after VNav indicated its location. In this case the error of the registration could be measured by determining the distance between the target point set in the CT- or MR-images and the center of the lesion visible on US.

2.7. Statistical analyses

For the statistical analyses SPSS version 23 (IBM SPSS Statistics, IBM Nederland BV, Amsterdam, the Netherlands) was used. The independent-samples *t*-test and ANOVA were used for comparison of mean values, the Fischer's exact test for comparing nominal variables. For comparison of the lesions between the guidance modalities *a*VNav and CT-guidance were combined; This group consisted of lesions that were not possible to ablate with either US-guidance or *m*VNav. A p-value

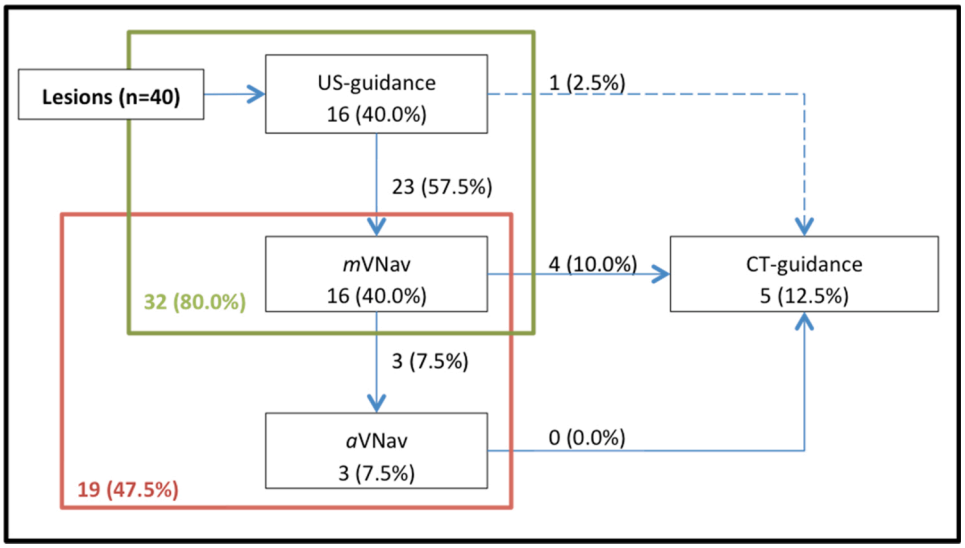

Fig. 2. Flowchart demonstrating the distribution of the lesions over the guidance modalities used for ablation. *The lesion shown with the dashed arrow was targeted under CT-guidance, because conventional US identification was complicated after a pneumothorax occurred during the first puncture.*

<0.05 was considered statistically significant.

3. Results

3.1. Application of interventional guidance approaches

Seventeen of 25 patients (68.0 %; n = 26 lesions) were treated with

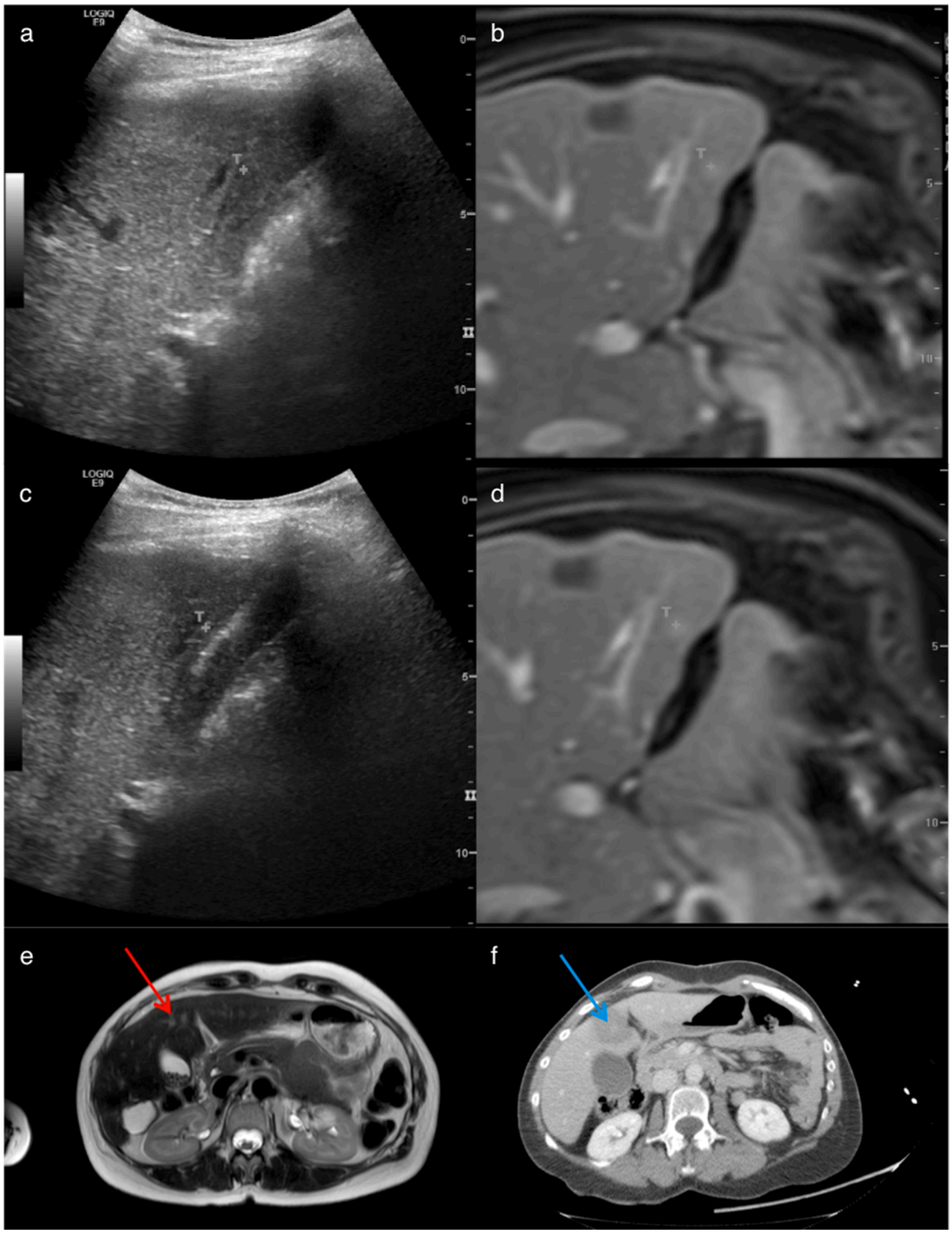

Fig. 3. Clinical examples of the value of VNav. Using *m*VNav the lesion could not be seen with conventional US imaging (a), even though they are compared with diagnostic MR images (b). However, a target was set on the lesion using the MR image and the target icon (T) appears on the US image as well. Now, VNav gives an indication of its location. An electrode was inserted (white arrows) towards the target under guidance of the *m*VNav (c and d). The pre-interventional MR images (e) are compared to the post-interventional CT-images (f). The lesion (red arrow) appears to be inside the ablation zone (blue arrow). (For interpretation of the references to colour in this figure legend, the reader is referred to the web version of this article).

RFA (15 with 3 cm and two with 4 cm exposure electrodes). Eight of 25 patients (32.0 %; n = 14 lesions) were treated with MWA.

Thirty-two of the 40 ablated lesions were ablated using a single applicator and eight using multiple applicators. Sixteen of 40 lesions (40.0 %) were targeted using conventional US-guidance, sixteen (40.0 %) were targeted using *m*VNav, three (7.5 %) using *a*VNav, and five (12.5 %) with CT-guidance (Fig. 2). One lesion that could be identified with conventional US was ablated under CT-guidance; a pneumothorax after the first puncture complicated further US identification (Fig. 2). Image data sets used for *m*VNav were derived from CT or MR (both in eight lesions). Post-ablation CE-CT showed an overall technical success rate of 95 % (38 of 40 lesions). This was 93.8 % (15/16) for conventional US-guidance, 100 % (16/16) for mVNav, 100 % (3/3) aVNav and 80 % (4/5) for CT-guidance.

23 of 40 lesions (57.5%; Fig. 2) were initially not visible on conventional US (n = 16; 40.0 %) or the interventionalist was uncertain about the location (n = 7; 17.5 %). The interventionalist was able to target 69.6 % (16 of 23) of these lesions with *m*VNav. This resulted in a two-fold increase in the number of lesions that could be targeted efficiently using US-guidance (80.0 % in total; Fig. 2).

To adjust the *m*VNav registration after plane-lock, the interventionalists used a median of three landmarks (range 1–4). In 56.3 % of the ablations performed using *m*VNav (9 of 16), the interventionalist placed the applicator(s) in the lesion only based on the virtual feedback provided by the navigation set-up (Fig. 3).

3.2. Lesion characteristics versus guidance modality

The mean size (± SD) of the lesions was 15.5 ± 8.7 mm (range 5.0–36.0 mm). Lesions targeted by *m*VNav (9.1 ± 4.6 mm) were significantly smaller than lesions targeted using conventional US-guidance (20.4 ± 9.4 mm, $p < 0.001$)(Fig. 4). The mean size of the lesions targeted by *a*VNav (16.7 ± 9.1 mm) or CT-guidance (19.5 ± 3.8 mm) did not differ from those targeted using conventional US-guidance ($p = 0.542$ and $p = 0.845$, respectively). In patients where *m*VNav was applied and the error could be measured, the mean navigation inaccuracy was 5.7 ± 2.3 mm (mean ± SD; range 3.00–9.00 mm; one missing value; seven lesions).

Comparison between the three guidance groups (conventional US-guidance, *m*VNav, or *a*VNav and CT-guidance) did, however, not reveal a clear difference in: 1) the distribution of lesion types ($p = 0.060$), 2) the presence of liver cirrhosis ($p = 0.801$), or 3) the anatomical location wherein the lesions occurred (measured over preference for segment 8 ($p = 0.360$), left or right lobe ($p = 0.409$), or the individual segments ($p = 0.221$)).

3.3. Follow up

Long-term follow-up revealed a recurrence rate of 52 % on patient basis at 29–33 months. Recurrence-free survival is shown in Fig. 5.

4. Discussion

This study emphasizes the value of *m*VNav on US-guided RF and MW ablations, for the complementary use of *m*VNav doubles the number (from 40 to 80 %) of US-guided ablations. In 69.6 % (16 of 23) of the lesions that could not be targeted using conventional US-guidance, the lesions could be targeted with *m*VNav, which is in line with the expectations expressed by Lee et al. [15]. Hence, *m*VNav may be considered a minimal invasive alternative for CT-guidance, resulting in less radiation exposure for the patient and interventionalist, lack of need for contrast medium, lower costs and improved logistics.

A small lesion size appeared the most frequent limitation of conventional US-guidance ablations and is in line with limitations found in other studies [3,12], however, *m*VNav supported the ablation of significantly smaller lesions. The mean size of the lesions ablated under *a*VNav or CT-guidance did not differ from the size of lesions ablated under conventional US-guidance, but were not able to be ablated with mVNav guidance. It is uncertain why this is the case, since there was no difference in the location of the lesions or presence of liver cirrhosis.

The amount of lesions that were not visible using conventional US-guidance (n = 16, 40.0 % in the total group) is in line with the 27 % invisibility rate reported by Kim et al. [2]. When the uncertainty of the interventionalist was also taken into account, the invisibility rate in this

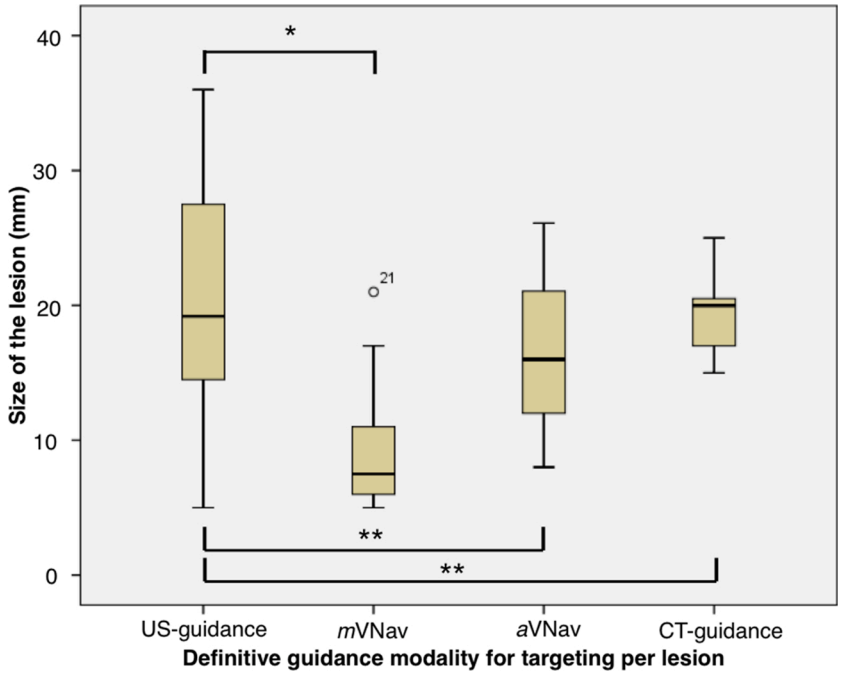

Fig. 4. Boxplot showing the distribution of the sizes of the lesions targeted with guidance of one of the four modalities. Mean size ± standard deviation per guidance modality: conventional US = 20.4 ± 9.4 mm; *m*VNav = 9.1 ± 4.6 mm; *a*VNav = 16.7 ± 9.1 mm; CT = 19.5 ± 3.8 mm. *$p < 0.001$. **Conventional US-guidance compared with *a*VNav or CT-guidance; $p = 0.542$ and $p = 0.845$, respectively.

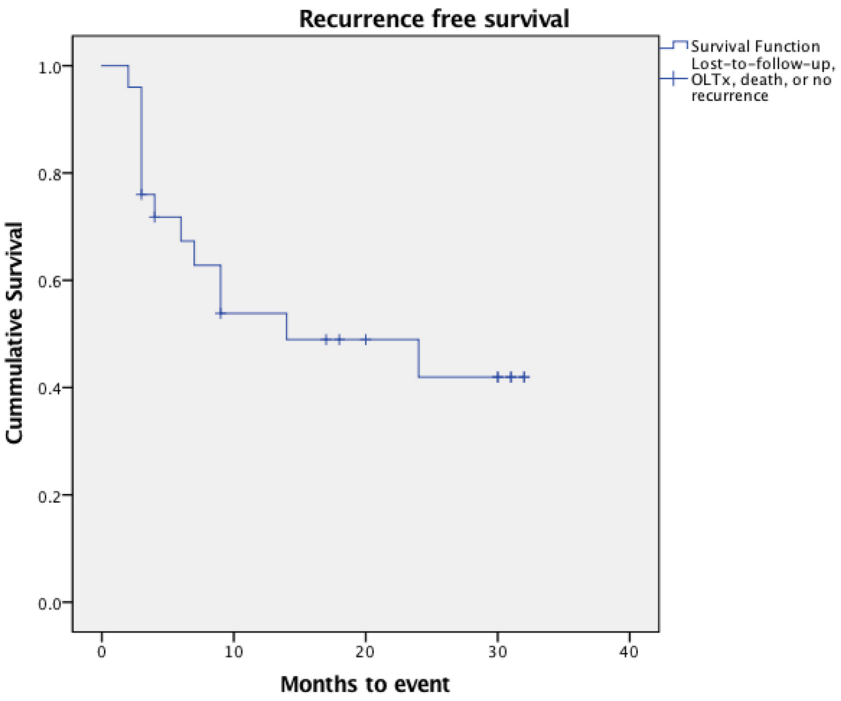

Fig. 5. Recurrence free survival.

study increased with 17.5 % (total of 57.5 %). Uncertainties are e.g. mistaking cirrhotic nodules for lesions (pseudolesions), or poor conspicuity of the lesion [26]. This is in line with 16.7 % of pseudolesions and 7.4 % of mistargeting reported earlier by Lee et al. [15].

The recurrence rate of 52 % found in this study also corresponds to the recurrence rate of 43.4 % and 59.8 % for 2 and 3 years follow-up reported by Tateishi et al. [27].

The registration method used for *m*VNav was based on plane-registration [28,29,23]. Plane registration can be considered a less accurate manual registration procedure compared to point-registration, however it was considered to be more practical [23], because identification of well-defined landmarks for point registration can be difficult in patients [30]. Use of an additional registration point allowed for refinement of the planar registration [30,23].

We found a registration error of 5.7 mm with *m*VNav which is in line with the 5.8 mm found by Krücker et al. (2007) [31].

The use of an active tracker in the *a*VNav set-up limited the chance of manual (human) error and reduced position artefacts encountered between the acquisition of the CT-scan used for navigation and the interventional setting. An obvious question that arises is: Which of the two navigation procedures, *m*VNav or *a*VNav, did we consider most valuable? The sequential order (US-guidance, *m*VNav, *a*VNav, CT-guidance) of the current study did not allow for a definite head-to-head comparison. However, the order itself already provides valuable information as *m*VNav is more easily applied as it does not require interventional CE-CT.

Although an explicit influence of the navigation was seen on the number of lesions that could be treated without CT, the current study was limited by its retrospective design and the limited number of patients included. To fully strengthen the current findings, a prospective study that evaluates VNav in ultrasonographically inconspicuous liver lesions in a large (randomized) group of patients is recommended. Furthermore, next to the impact navigation has on the number of lesions that can be successfully treated without CT guidance, it would also be very interesting to investigate the influence that such navigation has on the dexterity and decision-making of the interventional radiologist during the US-guided procedure. In different medical fields (e.g., surgery), such concepts are increasingly used to study the influence a technology has on the procedural performance of the specialist [32].

5. Conclusion

Integrating an *m*VNav set-up in our study doubled the number of lesions that could be treated using minimally-invasive US-guided ablation. *m*VNav also supported the treatment of smaller lesions. Evaluation of this technology in a larger patient cohort is recommended to strengthen these results.

Ethical approval

All procedures performed in studies involving human participants were in accordance with the ethical standards of the institutional and/or national research committee and with the 1964 Helsinki declaration and its later amendments or comparable ethical standards.

Informed consent

Informed consent was obtained from all individual participants included in the study.

Funding

This project was supported with an NWO TTW-VIDI grant from the Dutch Research Council (Grant No. STW BGT11272).

CRediT authorship contribution statement

Philippa Meershoek: Investigation, Writing - original draft, Visualization. **Nynke S. van den Berg:** Formal analysis, Writing - review & editing. **Jacob Lutjeboer:** Investigation, Writing - review & editing. **Mark C. Burgmans:** Investigation, Writing - review & editing. **Rutger W. van der Meer:** Investigation, Writing - review & editing. **Catharina S.P. van Rijswijk:** Investigation, Writing - review & editing. **Matthias N. van Oosterom:** Formal analysis, Writing - review & editing, Visualization. **Arian R. van Erkel:** Methodology, Supervision, Investigation, Writing - review & editing. **Fijs W.B. van Leeuwen:** Conceptualization,

Methodology, Supervision, Writing - original draft, Funding acquisition.

Declaration of Competing Interest

The authors declare that they have no conflict of interest.

Acknowledgments

We would like to acknowledge the interventional radiology staff for their help during this study.

Appendix A. Supplementary data

Supplementary material related to this article can be found, in the online version, at doi:https://doi.org/10.1016/j.ejro.2021.100367.

References

[1] S. Clasen, H. Rempp, R. Hoffmann, H. Graf, P.L. Pereira, C.D. Claussen, Image-guided radiofrequency ablation of hepatocellular carcinoma (HCC): is MR guidance more effective than CT guidance? Eur. J. Radiol. 83 (1) (2014) 111–116, https://doi.org/10.1016/j.ejrad.2013.09.018.

[2] J.E. Kim, Y.S. Kim, H. Rhim, H.K. Lim, M.W. Lee, D. Choi, S.W. Shin, S.K. Cho, Outcomes of patients with hepatocellular carcinoma referred for percutaneous radiofrequency ablation at a tertiary center: analysis focused on the feasibility with the use of ultrasonography guidance, Eur. J. Radiol. 79 (2) (2011), https://doi.org/10.1016/j.ejrad.2011.03.090 e80-84.

[3] P.N. Kim, D. Choi, H. Rhim, S.E. Rha, H.P. Hong, J. Lee, J.I. Choi, J.W. Kim, J. W. Seo, E.J. Lee, H.K. Lim, Planning ultrasound for percutaneous radiofrequency ablation to treat small (</= 3 cm) hepatocellular carcinomas detected on computed tomography or magnetic resonance imaging: a multicenter prospective study to assess factors affecting ultrasound visibility, J. Vasc. Interv. Radiol. 23 (5) (2012) 627–634, https://doi.org/10.1016/j.jvir.2011.12.026.

[4] G. Mauri, L. Cova, S. De Beni, T. Ierace, T. Tondolo, A. Cerri, S.N. Goldberg, L. Solbiati, Real-time US-CT/MRI image fusion for guidance of thermal ablation of liver tumors undetectable with US: results in 295 cases, Cardiovasc. Intervent. Radiol. 38 (1) (2015) 143–151, https://doi.org/10.1007/s00270-014-0897-y.

[5] T. Metz, A. Heider, R. Vellody, M.D. Jarboe, J.J. Gemmete, J.J. Grove, E.A. Smith, R. Mody, E.A. Newman, J.R. Dillman, Image-guided percutaneous core needle biopsy of soft-tissue masses in the pediatric population, Pediatr. Radiol. (2016), https://doi.org/10.1007/s00247-016-3571-5.

[6] H. Rhim, H.K. Lim, Kim Y-s, D. Choi, W.J. Lee, Radiofrequency ablation of hepatic tumors: lessons learned from 3000 procedures, J. Gastroenterol. Hepatol. 23 (10) (2008) 1492–1500, https://doi.org/10.1111/j.1440-1746.2008.05550.x.

[7] J.Y. Lee, B.I. Choi, Y.E. Chung, M.W. Kim, S.H. Kim, J.K. Han, Clinical value of CT/MR-US fusion imaging for radiofrequency ablation of hepatic nodules, Eur. J. Radiol. 81 (9) (2012) 2281–2289, https://doi.org/10.1016/j.ejrad.2011.08.013.

[8] K.D. Song, M.W. Lee, H. Rhim, D.I. Cha, Y. Chong, H.K. Lim, Fusion imaging-guided radiofrequency ablation for hepatocellular carcinomas not visible on conventional ultrasound, AJR Am. J. Roentgenol. 201 (5) (2013) 1141–1147, https://doi.org/10.2214/ajr.13.10532.

[9] M.W. Lee, Y.J. Kim, H.S. Park, Jung S.I. Yu NC, S.Y. Ko, H.J. Jeon, Targeted sonography for small hepatocellular carcinoma discovered by CT or MRI: factors affecting sonographic detection, AJR Am. J. Roentgenol. 194 (5) (2010), https://doi.org/10.2214/ajr.09.3171. W396-400.

[10] N. Toshikuni, M. Tsutsumi, Y. Takuma, T. Arisawa, Real-time image fusion for successful percutaneous radiofrequency ablation of hepatocellular carcinoma, J. Ultrasound Med. 33 (11) (2014) 2005–2010, https://doi.org/10.7863/ultra.33.11.2005.

[11] L. Crocetti, C. Della Pina, D. Cioni, R. Lencioni, Peri-intraprocedural imaging: US, CT, and MRI, Abdom. Imaging 36 (6) (2011) 648–660, https://doi.org/10.1007/s00261-011-9750-9.

[12] H. Rhim, M.H. Lee, Y.S. Kim, D. Choi, W.J. Lee, H.K. Lim, Planning sonography to assess the feasibility of percutaneous radiofrequency ablation of hepatocellular carcinomas, AJR Am. J. Roentgenol. 190 (5) (2008) 1324–1330, https://doi.org/10.2214/ajr.07.2970.

[13] Baère Td, C. Dromain, M. Lapeyre, P. Briggs, J.S. Duret, A. Hakime, V. Boige, M. Ducreux, Artificially Induced Pneumothorax for Percutaneous Transthoracic Radiofrequency Ablation of Tumors in the Hepatic Dome: Initial Experience, Radiology 236 (2) (2005) 666–670, doi:doi:10.1148/radiol.2362040992.

[14] T.W. Kang, H. Rhim, Recent advances in tumor ablation for hepatocellular carcinoma, Liver Cancer 4 (3) (2015) 176–187, https://doi.org/10.1159/000367740.

[15] M.W. Lee, H. Rhim, D.I. Cha, Y.J. Kim, D. Choi, Y.J.S. Kim, H.K. Lim, Percutaneous radiofrequency ablation of hepatocellular carcinoma: fusion imaging guidance for management of lesions with poor conspicuity at conventional sonography, AJR Am. J. Roentgenol. 198 (6) (2012) 1438–1444, https://doi.org/10.2214/ajr.11.7568.

[16] Y. Makino, Y. Imai, T. Igura, S. Kogita, Y. Sawai, K. Fukuda, M. Hori, M. Kudo, T. Murakami, Usefulness of the extracted-overlay function in CT/MR-ultrasonography fusion imaging for radiofrequency ablation of hepatocellular carcinoma, Dig. Dis. 31 (5–6) (2013) 485–489, https://doi.org/10.1159/000355257.

[17] G.H. KleinJan, N.S. van den Berg, M.N. van Oosterom, T. Wendler, M. Miwa, A. Bex, K. Hendricksen, S. Horenblas, F.W. van Leeuwen, Towards (hybrid) navigation of a fluorescence camera in an open surgery setting, J. Nucl. Med. (2016), https://doi.org/10.2967/jnumed.115.171645.

[18] M.N. van Oosterom, M.A. Engelen, N.S. van den Berg, G.H. KleinJan, H.G. van der Poel, T. Wendler, C.J. van de Velde, N. Navab, F.W. van Leeuwen, Navigation of a robot-integrated fluorescence laparoscope in preoperative SPECT/CT and intraoperative freehand SPECT imaging data: a phantom study, J. Biomed. Opt. 21 (8) (2016), https://doi.org/10.1117/1.jbo.21.8.086008, 86008.

[19] W.H. Nam, D.G. Kang, D. Lee, J.Y. Lee, J.B. Ra, Automatic registration between 3D intra-operative ultrasound and pre-operative CT images of the liver based on robust edge matching, Phys. Med. Biol. 57 (1) (2012) 69–91, https://doi.org/10.1088/0031-9155/57/1/69.

[20] D. Spinczyk, Towards the clinical integration of an image-guided navigation system for percutaneous liver tumor ablation using freehand 2D ultrasound images, Comput. Aided Surg. 20 (1) (2015) 61–72, https://doi.org/10.3109/10929088.2015.1076043.

[21] W. Wein, S. Brunke, A. Khamene, M.R. Callstrom, N. Navab, Automatic CT-ultrasound registration for diagnostic imaging and image-guided intervention, Med. Image Anal. 12 (5) (2008) 577–585, https://doi.org/10.1016/j.media.2008.06.006.

[22] B.J. Wood, J. Kruecker, N. Abi-Jaoudeh, J. Locklin, E. Levy, S. Xu, L. Solbiati, A. Kapoor, H. Amalou, A. Venkatesan, Navigation systems for ablation, J. Vasc. Interv. Radiol. 21 (8 Suppl) (2010), https://doi.org/10.1016/j.jvir.2010.05.003. S257-263.

[23] M.C. Burgmans, J.M. den Harder, P. Meershoek, N.S. van den Berg, S. Chan, F.W. B. van Leeuwen, A.R. van Erkel, Phantom Study Investigating the Accuracy of Manual and Automatic Image Fusion with the GE Logiq E9: Implications for use in Percutaneous Liver Interventions, Cardiovasc. Intervent. Radiol. 40 (6) (2017) 914–923, https://doi.org/10.1007/s00270-017-1607-3.

[24] Mc Burgmans, Cw Too, M. Fiocco, Aj Kerbert, Rh Lo, Jj Schaapman, Ar van Erkel, Mj Coenraad, Bs Tan, Differences in patient characteristics and midterm outcome between asian and european patients treated with radiofrequency ablation for hepatocellular carcinoma, Cardiovasc. Intervent. Radiol. 39 (12) (2016) 1708–1715, https://doi.org/10.1007/s00270-016-1462-7.

[25] M. Ahmed, L. Solbiati, C.L. Brace, D.J. Breen, M.R. Callstrom, J.W. Charboneau, M. H. Chen, B.I. Choi, T. de Baere, G.D. Dodd 3rd., D.E. Dupuy, D.A. Gervais, D. Gianfelice, A.R. Gillams, F.T. Lee Jr., E. Leen, R. Lencioni, P.J. Littrup, T. Livraghi, D.S. Lu, J.P. McGahan, M.F. Meloni, B. Nikolic, P.L. Pereira, P. Liang, H. Rhim, S.C. Rose, R. Salem, C.T. Sofocleous, S.B. Solomon, M.C. Soulen, M. Tanaka, T.J. Vogl, B.J. Wood, S.N. Goldberg, Image-guided tumor ablation: standardization of terminology and reporting criteria–a 10-year update, J. Vasc. Interv. Radiol. 25 (11) (2014) 1691–1705, https://doi.org/10.1016/j.jvir.2014.08.027, e1694.

[26] M.W. Lee, H.K. Lim, Y.J. Kim, D. Choi, Y.J.S. Kim, M.W.J. Lee, D.I. Cha, M.J. Park, H. Rhim, Percutaneous sonographically guided radio frequency ablation of hepatocellular carcinoma: causes of mistargeting and factors affecting the feasibility of a second ablation session, J. Ultrasound Med. 30 (5) (2011) 607–615.

[27] R. Tateishi, S. Shiina, T. Teratani, S. Obi, S. Sato, Y. Koike, T. Fujishima, H. Yoshida, T. Kawabe, M. Omata, Percutaneous radiofrequency ablation for hepatocellular carcinoma. An analysis of 1000 cases, Cancer 103 (6) (2005) 1201–1209, https://doi.org/10.1002/cncr.20892.

[28] Y. Makino, Y. Imai, T. Igura, H. Ohama, S. Kogita, Y. Sawai, K. Fukuda, H. Ohashi, T. Murakami, Usefulness of the multimodality fusion imaging for the diagnosis and treatment of hepatocellular carcinoma, Dig. Dis. 30 (6) (2012) 580–587, https://doi.org/10.1159/000343070.

[29] Y. Minami, H. Chung, M. Kudo, S. Kitai, S. Takahashi, T. Inoue, K. Ueshima, H. Shiozaki, Radiofrequency ablation of hepatocellular carcinoma: value of virtual CT sonography with magnetic navigation, AJR Am. J. Roentgenol. 190 (6) (2008), https://doi.org/10.2214/ajr.07.3092. W335-341.

[30] C. Ewertsen, K. Ellegaard, M. Boesen, S. Torp-Pedersen, M. Bachmann Nielsen, Comparison of two co-registration methods for real-time ultrasonography fused with MRI: a phantom study, Ultraschall Med. 31 (3) (2010) 296–301, https://doi.org/10.1055/s-0029-1245457.

[31] J. Krucker, S. Xu, N. Glossop, A. Viswanathan, J. Borgert, H. Schulz, B.J. Wood, Electromagnetic tracking for thermal ablation and biopsy guidance: clinical evaluation of spatial accuracy, J. Vasc. Interv. Radiol. 18 (9) (2007) 1141–1150, https://doi.org/10.1016/j.jvir.2007.06.014.

[32] S. Azargoshasb, S. van Alphen, L.J. Slof, G. Rosiello, S. Puliatti, S.I. van Leeuwen, K.M. Houwing, M. Boonekamp, J. Verhart, P. Dell'Oglio, J. van der Hage, M.N. van Oosterom, F.W.B. van Leeuwen, The Click-On gamma probe, a second-generation tethered robotic gamma probe that improves dexterity and surgical decision-making, Eur. J. Nucl. Med. Mol. Imaging (2021), https://doi.org/10.1007/s00259-021-05387-z.